

Article

The Effect of Temperature on the Surface Energetic Properties of Carbon Fibers Using Inverse Gas Chromatography

Tayssir Hamieh ^{1,2} 

¹ Faculty of Science and Engineering, Maastricht University, P.O. Box 616, 6200 MD Maastricht, The Netherlands; t.hamieh@maastrichtuniversity.nl

² Laboratory of Materials, Catalysis, Environment and Analytical Methods (MCEMA), Faculty of Sciences, Lebanese University, Hadath P.O. Box 6573, Lebanon

Abstract: This paper constitutes an original and new methodology for the determination of the surface properties of carbon fibers in two forms, namely, oxidized and untreated, using the inverse gas chromatography technique at infinite dilution based on the effect of temperature on the surface area of various organic molecules adsorbed on the carbon fibers. The studied thermal effect showed a large deviation from the classical methods or models relative to the new determination of the surface properties of carbon fibers, such as the dispersive component of their surface energy, the free surface energy, the free specific energy, and the enthalpy and entropy of the adsorption of molecules on the carbon fibers. It was highlighted that the variations in the London dispersive surface energy of the carbon fibers as a function of the temperature satisfied excellent linear variations by showing large deviations between the values of $\gamma_s^d(T)$, calculated using different models, which can reach 300% in the case of the spherical model. All models and chromatographic methods showed that the oxidized carbon fibers gave larger specific free enthalpy of adsorption whatever the adsorbed polar molecules. The obtained specific enthalpy and entropy of the adsorption of the polar solvents led to the determination of the Lewis acid–base constants of the carbon fibers. Different molecular models and chromatographic methods were used to quantify the surface thermodynamic properties of the carbon fibers, and the results were compared with those of the thermal model. The obtained results show that the oxidized carbon fibers gave more specific interaction energy and greater acid–base constants than the untreated carbon fibers, thus highlighting the important role of oxidization in the acid–base of fibers. The determination of the specific acid–base surface energy of the two carbon fibers showed greater values for the oxidized carbon fibers than for the untreated carbon fibers. An important basic character was highlighted for the two studied carbon fibers, which was larger than the acidic character. It was observed that the carbon fibers were 1.4 times more acidic and 2.4 times more basic. The amphoteric character of the oxidized fibers was determined, and it was 1.7 times more important than that of the untreated fibers. This tendency was confirmed by all molecular models and chromatographic methods. The Lewis acid and base surface energies of the solid surface, γ_s^+ and γ_s^- , as well as the specific acid–base surface energy γ_s^{AB} of the carbon fibers at different temperatures were determined. One showed that the specific surface energy γ_s^{AB} of the oxidized fibers was 1.5 times larger than that of the untreated fibers, confirming the above results obtained on the strong acid–base interactions of the oxidized carbon fibers with the various polar molecules.

Keywords: dispersive surface energy; specific acid–base surface energy; specific surface enthalpy and entropy of adsorption; Lewis acid–base enthalpic and entropic constants; thermal effect



Citation: Hamieh, T. The Effect of Temperature on the Surface Energetic Properties of Carbon Fibers Using Inverse Gas Chromatography. *Crystals* **2024**, *14*, 28. <https://doi.org/10.3390/cryst14010028>

Academic Editor: Rajratan Basu

Received: 28 November 2023

Revised: 16 December 2023

Accepted: 20 December 2023

Published: 26 December 2023



Copyright: © 2023 by the author. Licensee MDPI, Basel, Switzerland. This article is an open access article distributed under the terms and conditions of the Creative Commons Attribution (CC BY) license (<https://creativecommons.org/licenses/by/4.0/>).

1. Introduction

Carbon fibers exhibit excellent physicochemical and mechanical properties, and they are used as alternatives to conventional metals for various applications, especially for decreasing the weight of conventional products. The technical progress of carbon fibers has

led to an enhanced elastic modulus by increasing the size of crystals and arranging them along the fiber axis [1].

Carbon fibers are chemically inert materials and are not influenced by air, humidity, weak acids, alkalis or solvents at ambient temperatures. Nevertheless, they suffer from oxidation at higher temperatures [2]. Carbon fibers are mostly composed of carbon atoms (from 92% to 99% carbon). They are extremely stiff, possess high tensile strength and low weight and exhibit excellent resistance to chemical corrosion. Their low thermal expansion is an excellent advantage in different applications requiring good stability [1]. The science and technology of carbon fiber production has been well developed in the literature [2–5].

These interesting properties have made carbon fibers very popular in aerospace applications, civil engineering, the military and motorsports, along with other competitive sports. However, they are relatively expensive when compared with similar fibers, such as plastic fibers. The exceptional mechanical properties of carbon fibers are advantageously used in composite applications, where their low weight is an excellent factor in some industrial applications, such as aerospace sectors, the military, turbine blades, construction, lightweight cylinders and pressure vessels, off-shore tethers and drilling risers, medicine, automobiles and sporting goods.

In recent years, the carbon fiber industry has been growing steadily to meet the demand from different industries, such as the aerospace industry (aircraft and space systems), the military, turbine blades, construction (non-structural and structural systems), lightweight cylinders and pressure vessels, off-shore tethers and drilling risers, medicine, automobiles and sporting goods [6–12]. For the automotive industry, fiber-reinforced polymeric composites offer reduced weight and superior styling. Carbon fibers can find applications in body parts (doors, hoods, deck lids, front end, bumpers, etc.), chassis and suspension systems (e.g., leaf springs), drive shafts and so on [12].

The large specific surface area, controllable chemical compositions, excellent electrical conductivity and rich composite forms of carbon fibers are promising for future applications in energy conversion technologies and new challenges and prospects for fiber materials in electrocatalysis applications [13].

Many authors were previously interested in the characterization of the dispersive and specific interactions of carbon fibers using inverse gas chromatography (IGC) at infinite dilution and, more particularly, by determining the surface physicochemical properties of carbon fibers, such as their dispersive component of surface energy, their free energy of adsorption and their specific enthalpy and entropy of the adsorption of some model organic molecules on the carbon fibers [4,5,12–16]. Other recent studies were devoted to determining the effect of oxidation temperature on some commercial carbon fibers [17] or to optimizing the testing conditions of various carbon fiber bundles [18]. Pala et al. [19] studied the surface energy and acid–base properties of some highly porous activated carbons by using inverse gas chromatography. However, the values of different surface thermodynamic parameters previously obtained by different authors [4,5,12–16] using classic chromatographic methods were recently criticized in the literature [20–24]. The effect of the temperature of organic solvents on the surface properties of carbon fibers has never been studied.

Because of the extreme importance of the physicochemical properties of carbon fibers in many different industrial applications, in this paper, we are interested in the correction of the various surface parameters of carbon fibers in two forms, namely, untreated and oxidized, by taking into account the recent progress in the inverse gas chromatography technique.

2. IGC Methods and Models

2.1. Classical Methods

Many papers have been devoted to the determination of the surface physicochemical properties and the Lewis acid–base parameters of solid surfaces in both powder and fiber forms by using the IGC technique at infinite dilution [25–36]. Such studies concentrated on the determination of the dispersive surface energy and the specific energy, and the

enthalpy and entropy of the adsorption of n-alkanes and polar molecules on oxides, metals or polymers. To that end, several methods were used. These various methods were based on the linear relations found between the free energy of adsorption $\Delta G_a(T)$ or $RT\ln(Vn)$ (at various values of temperature T) as a function of certain reference thermodynamic parameters, where R is the ideal gas constant, and Vn the net retention volume of the injected probes into a chromatographic column containing the solid substrate. In the IGC technique, polar or non-polar organic solvents were used. The used non-polar molecules were the n-alkanes (from n-pentane C5 to n-decane C10) describing the dispersive properties of the solid surfaces. In general, polar solvents comprise the following: acetone, ethyl acetate, ethyl oxide, toluene, benzene, acetonitrile, ethanol, propanol, carbon tetrachloride, chloroform and dichloromethane.

Different reference thermodynamic parameters were used:

- The boiling point $T_{B.P.}$ of the solvents [25];
- The vapor pressure P_0 of the probes at a fixed temperature [26,27];
- The dispersive component γ_l^d of the surface energy of the solvent [14];
- The deformation polarizability α_0 [28];
- The standard enthalpy of the vaporization ΔH_{vap}^0 (supposed constant) of the organic molecules [29,30];
- The topological index χ_T of the solvents [31,32].

New molecular models and IGC methods [20–22] were proposed based on the linear dependency of $RT\ln(Vn)$ obtained from IGC measurements, with respect to any of the thermodynamic parameters X_j of organic molecules.

By varying the temperature of the column, one can obtain the values of the specific free energy $\Delta G_a^{sp}(T)$ of polar molecules adsorbed on solid surfaces by calculating the distance relating the representative point of $RT\ln(Vn)$ of a polar molecule to its hypothetical point located on the n-alkane straight line. The specific enthalpy ΔH_a^{sp} and entropy ΔS_a^{sp} of the adsorbed polar molecule are then deduced from relation (1):

$$\Delta G_a^{sp}(T) = \Delta H_a^{sp} - T \Delta S_a^{sp} \quad (1)$$

And, consequently, one obtains the acid–base constants K_A and K_D of the solids from the following relation [26,27]:

$$\frac{-\Delta H^{sp}}{AN} = \frac{DN}{AN} K_A + K_D \quad (2)$$

where AN and DN respectively represent the electron donor and acceptor numbers of the polar molecule given by Gutmann [33] and corrected by Fowkes.

However, we can determine the dispersive component γ_s^d of the surface energy of a solid surface by using the method of Dorris–Gray [34] based on Fowkes's relation [35]. The obtained relation giving $\gamma_s^d(T)$ is the following:

$$\gamma_s^d = \frac{\left[RT\ln \left[\frac{V_n(C_{n+1}H_{2(n+2)})}{V_n(C_nH_{2(n+1)})} \right] \right]^2}{4N^2 a_{-CH_2-}^2 - \gamma_{-CH_2-}} \quad (3)$$

where $C_nH_{2(n+1)}$ and $C_{n+1}H_{2(n+2)}$ are two consecutive n-alkanes; a_{-CH_2-} is the surface area of the methylene group, with $a_{-CH_2-} = 6 \text{ \AA}$ independent of the temperature; and the surface energy γ_{-CH_2-} is equal to γ_{-CH_2-} (in mJ/m^2) = $52.603 - 0.058T$ (T in K).

Another equivalent method was proposed in the literature [14], and it allows for the determination of γ_s^d of solid surfaces by using the following relation:

$$RT\ln(Vn) = 2Na \left(\gamma_l^d \gamma_s^d \right)^{1/2} + \alpha(T) \quad (4)$$

where a is the surface area of an adsorbed molecule (previously supposed constant), \mathcal{N} is the Avogadro number, and $\alpha(T)$ is a constant depending only on the temperature and the solid substrate.

2.2. Recent Progress

2.2.1. Molecular Models

The values of the dispersive surface energy γ_s^d of solid substrates proposed by relations (3) and (4) were obtained by supposing that the surface areas of the methylene group and the organic molecules are constant independent of the temperature. It was also supposed that γ_l^d is constant. In previous works [24], one proposed different molecular models allowing the determination of the surface areas of molecules:

- Kiselev results;
- Two-dimensional Van der Waals (VDW) equation;
- Two-dimensional Redlich–Kwong (R-K) equation;
- Geometric model based on the real form of molecules;
- Cylindrical model based on cylindrical form of molecules;
- Spherical model based on spherical form of molecules.

Table S1 gives the surface areas of n-alkanes for the different molecular models. Furthermore, the dispersive component of the surface tension of the solvents depended on the temperature.

2.2.2. Hamieh Thermal Model

In recent studies, one showed that the surface area of molecules extremely depends on the temperature [20–22]. Consequently, the new results will correct the values of γ_s^d , ΔG_a^{sp} and the Lewis acid–base constants. Indeed, new expressions for the surface area $a(T)$ of organic molecules and n-alkanes were proposed as a function of the temperature. It was also determined that the surface area of methylene group $a_{-CH_2-}(T)$ depends on the temperature [20–22]. One also showed that γ_l^d linearly depends on the temperature.

These new findings allowed us to determine the surface thermodynamic properties of carbon fibers by using all classical IGC methods and the molecular models of the surface areas of molecules. The values of the surface parameters obtained using the classical methods were corrected by our new thermal model taking into account the variations in the surface areas and $\gamma_l^d(T)$ of organic molecules as a function of the temperature. In Table S2, we give the expressions of $\gamma_l^d(T)$ of n-alkanes.

3. Experimental Section

3.1. Materials and Solvents

All used n-alkanes (hexane, heptane, octane, nonane) and polar solvents, of highly pure grade (99%), were purchased from Fisher Scientific (Lebanon, Beirut). The used polar molecules were, in Lewis terms, acidic, such as carbon tetrachloride (CCl_4), chloroform (CHCl_3) and dichloromethane (CH_2Cl_2); amphoteric, such as acetone; basic, such as ethyl acetate, diethyl ether and tetrahydrofuran (THF); and weak amphoteric, such as benzene. Two carbon fibers were analyzed: untreated fibers and oxidized fibers. The corrected acceptor number and normalized donor number of the electrons of the polar solvents are given in Table S3.

3.2. GC Conditions

Experimental measurements were performed on a commercial Focus GC gas chromatograph equipped with a flame ionization detector. The carbon fibers were filled into a stainless-steel column with a 2 mm inner diameter and a length of 20 cm. The temperature range varied from 40 °C to 100 °C. The different experimental conditions are typically the same as those given in previous published papers [20–22]. The column was packed with 1 g of carbon fibers with a diameter of 10 mm and a length of 50 cm. The standard deviation of the obtained retention time, t_R , was less than 1% in all measurements.

3.3. Results

3.3.1. Dispersive Component of Surface Energy of Carbon Fibers

All previous various molecular models and the Dorris–Gray method were used to determine the dispersive component of the surface energy of the carbon fibers (untreated and oxidized). The results were compared to those obtained using the thermal model [20–22] (Figure 1). The variations in $\gamma_s^d(T)$ of the carbon fibers as a function of the temperature satisfied excellent linear variations. Figure 1 shows large deviations between the values of $\gamma_s^d(T)$ calculated using the different models, which can reach 300% in the case of the spherical model. The application of the Dorris–Gray relation gave large values of $\gamma_s^d(T)$ in the case of the thermal model. The most accurate results were obtained using the thermal model [20–22]. One observed that the results of the thermal model (by using the results on PE) were very close to those of the cylindrical, Kiselev, Dorris–Gray and VDW models, whereas the average values gave similar results to those of the thermal model (on PTFE). Furthermore, a comparison between the dispersive surface energy of the carbon fiber types showed small differences not exceeding 10% in all used molecular models. One found a weaker decrease in $\gamma_s^d(T)$ in the case of the oxidized carbon fiber.

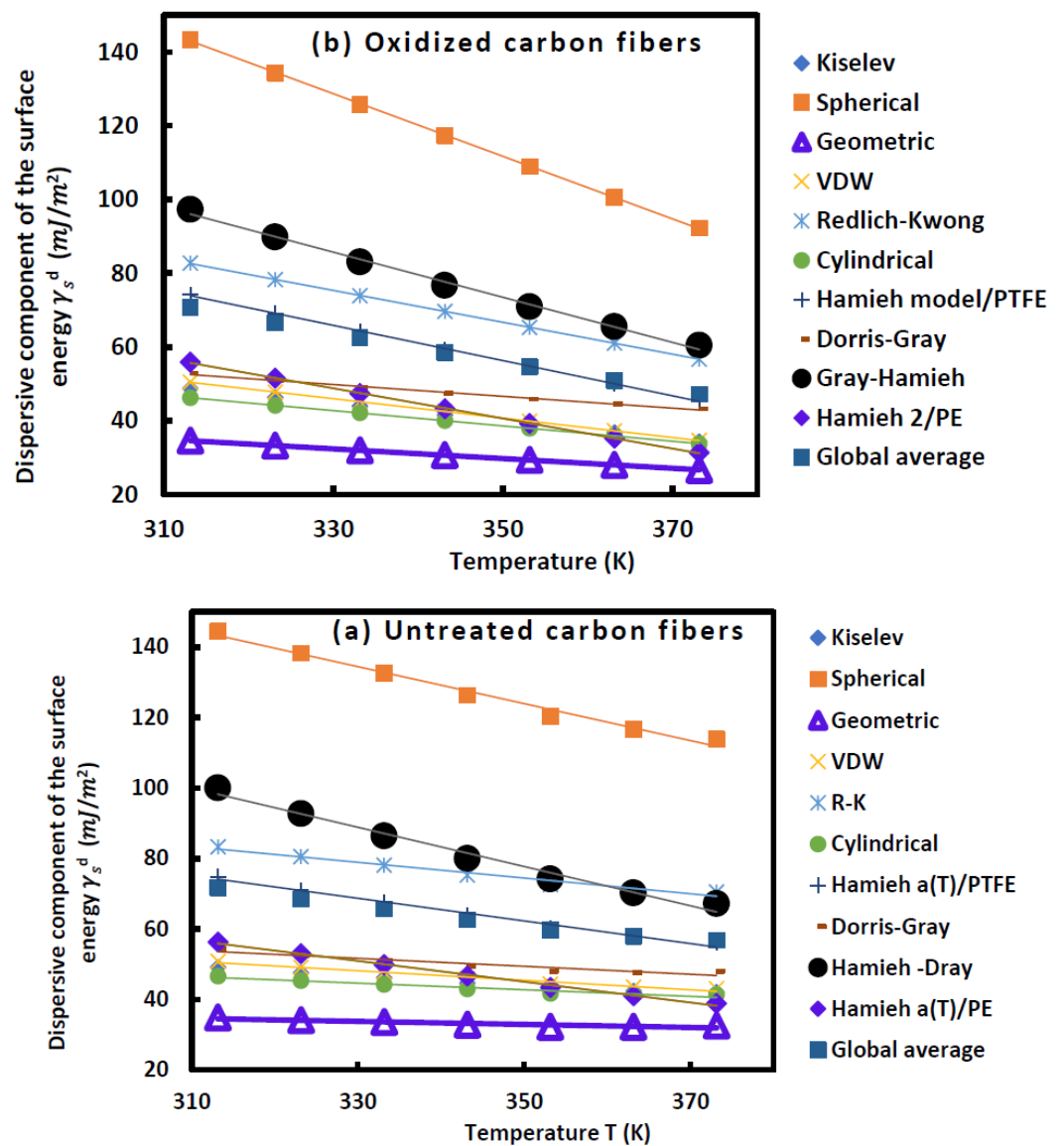


Figure 1. Evolution of γ_s^d (mJ/m^2) of carbon fibers, untreated (a) and oxidized (b), as a function of the temperature T (K) for the various molecular models.

Table 1 shows the various equations of $\gamma_s^d(T)$ relative to the carbon fibers for all used molecular models. Other new surface parameters were deduced and are presented below:

- The dispersive surface entropy ε_s^d , given by $\varepsilon_s^d = d\gamma_s^d/dT$
- The extrapolated values $\gamma_s^d(T = 0 \text{ K})$ at 0 K;
- The maximum temperature T_{Max} defined by $T_{Max} = -\frac{\gamma_s^d(T=0 \text{ K})}{\varepsilon_s^d}$.

Table 1. Equations $\gamma_s^d(T)$ of carbon fibers, untreated (a) and oxidized (b), for the different molecular models of n-alkanes, ε_s^d , $\gamma_s^d(T = 0 \text{ K})$ and T_{Max} .

Untreated Carbon Fibers (a)				
Molecular Model	$\gamma_s^d(T)$ (mJ/m^2)	$\varepsilon_s^d = d\gamma_s^d/dT$ ($\text{mJ m}^{-2} \text{ K}^{-1}$)	$\gamma_s^d(T = 0\text{K})$ (mJ/m^2)	T_{Max} (K)
Kiselev	$\gamma_s^d(T) = -0.13T + 88.0$	-0.13	88.0	702
Spherical	$\gamma_s^d(T) = -0.53T + 307.5$	-0.52	307.5	586
Geometric	$\gamma_s^d(T) = -0.07T + 55.3$	-0.07	55.3	848
VDW	$\gamma_s^d(T) = -0.14T + 92.7$	-0.14	92.7	686
Redlich–Kwong	$\gamma_s^d(T) = -0.22T + 152.5$	-0.22	152.5	684
Cylindrical	$\gamma_s^d(T) = -0.11T + 80.6$	-0.11	80.6	739
Hamieh a(T)/PTFE	$\gamma_s^d(T) = -0.32T + 174.7$	-0.32	174.7	544
Dorris–Gray	$\gamma_s^d(T) = -0.16T + 104.0$	-0.16	104.0	655
Hamieh–Gray	$\gamma_s^d(T) = -0.56T + 272.5$	-0.56	272.5	490
Hamieh a(T)/PE	$\gamma_s^d(T) = -0.29T + 148.2$	-0.29	148.2	503
Global average	$\gamma_s^d(T) = -0.26T + 151.2$	-0.26	151.2	590
Oxidized Carbon Fibers (b)				
Molecular Model	$\gamma_s^d(T)$ (mJ/m^2)	$\varepsilon_s^d = d\gamma_s^d/dT$ ($\text{mJ m}^{-2} \text{ K}^{-1}$)	$\gamma_s^d(T = 0\text{K})$ (mJ/m^2)	T_{Max} (K)
Kiselev	$\gamma_s^d(T) = -0.24T + 123.7$	-0.24	123.7	517
Spherical	$\gamma_s^d(T) = -0.52T + 307.5$	-0.52	307.5	586
Geometric	$\gamma_s^d(T) = -0.13T + 75.8$	-0.13	75.8	576
VDW	$\gamma_s^d(T) = -0.26T + 132.9$	-0.26	132.9	505
Redlich–Kwong	$\gamma_s^d(T) = -0.43T + 218.0$	-0.43	218.0	504
Cylindrical	$\gamma_s^d(T) = -0.21T + 111.3$	-0.21	111.3	536
Hamieh a(T)/PTFE	$\gamma_s^d(T) = -0.48T + 223.5$	-0.48	223.5	468
Dorris–Gray	$\gamma_s^d(T) = -0.16T + 102.7$	-0.16	102.7	641
Hamieh–Gray	$\gamma_s^d(T) = -0.61T + 287.6$	-0.61	287.6	470
Hamieh a(T)/PE	$\gamma_s^d(T) = -0.41T + 183.6$	-0.41	183.6	449
Global average	$\gamma_s^d(T) = -0.36T + 182.5$	-0.36	182.5	511

Table 1 shows that the dispersive surface entropy ε_s^d representing the slope of the straight line of $\gamma_s^d(T)$ negatively increased in the case of the oxidized carbon fibers by about 30% for all molecular models, proving a stronger decrease in $\gamma_s^d(T)$ of the treated fibers when the temperature increased but characterized by a smaller maximum temperature T_{Max} .

By applying the new thermal model, one confirmed a difference between the values of the maximum temperature T_{Max} of the two carbon fibers (a) and (b) approaching 500 K.

3.3.2. Specific Variables of Adsorption and Lewis Acid–Base Constants

The experimental chromatographic results allowed for the determination of the retention time and retention volume of the n-alkanes and polar solvents adsorbed on the two carbon fibers (a) and (b). Tables S4 and S5 show the values of $RT\ln(Vn)$ of the different solvents as a function of the temperature, and the evolution is represented in Figures S1 and S2. The results shown in Tables S4 and S5 and Figures S1 and S2 clearly show that the oxidized carbon fibers (b) gave greater values of $RT\ln(Vn)$ and therefore exhibited larger interactions than the untreated carbon fibers (a). One also observed an excellent linearity of the curves representing $RT\ln(Vn)$ versus the temperature for the different n-alkanes and polar solvents.

In order to quantify the specific interactions of the two fibers, one determined the values of the specific free energy ($\Delta G_a^{sp}(T)$) of the polar solvents adsorbed on the fibers as a function of the temperature (Tables S6 and S7), showing linear variations in ($\Delta G_a^{sp}(T)$) and dispersed values depending on the chromatographic methods and molecular models used. Figure 2 shows two examples of the results obtained with the diethyl ether, showing the large difference in ($\Delta G_a^{sp}(T)$) obtained when using the different molecular models and IGC methods in the two studied cases of carbon fibers.

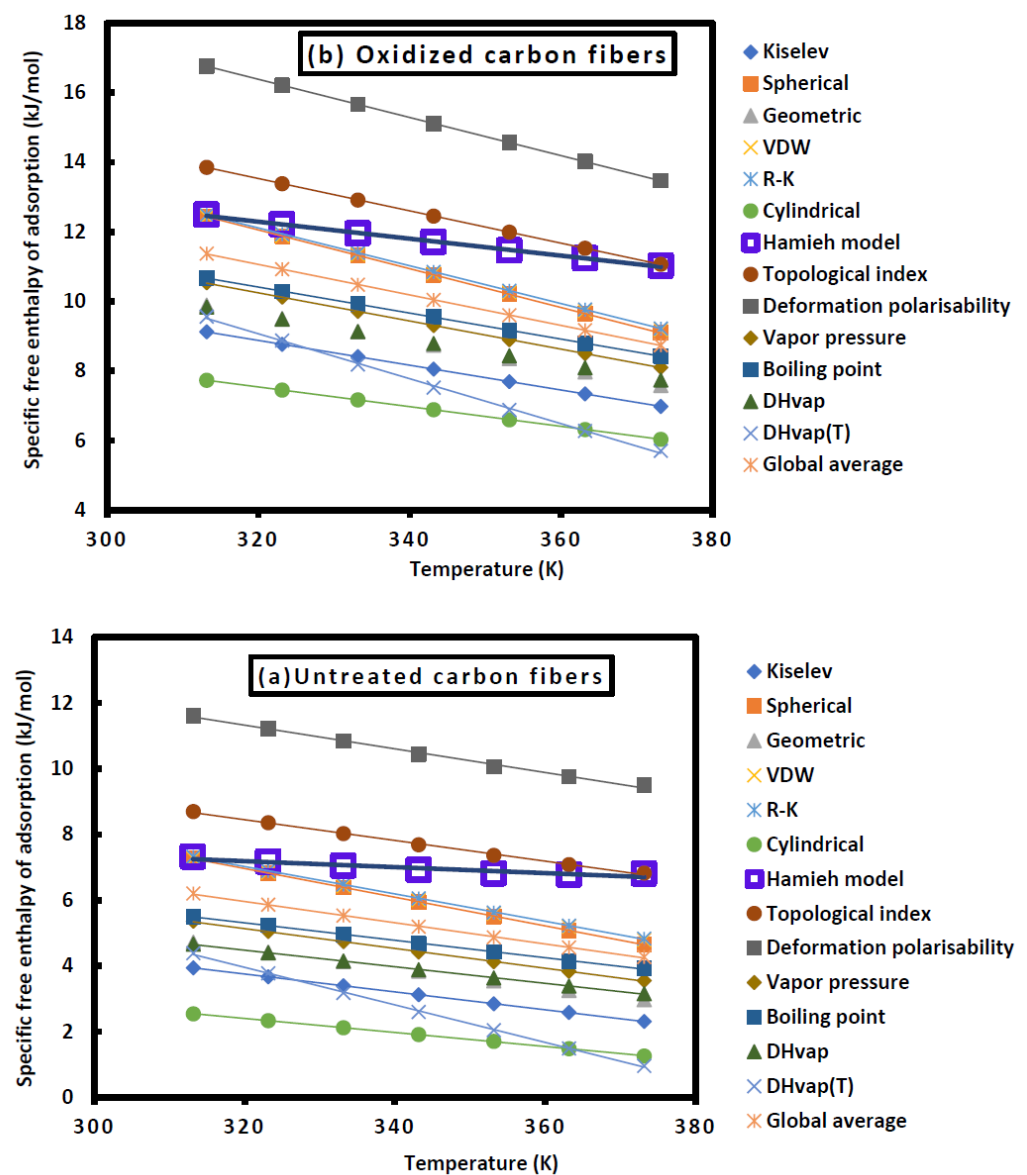


Figure 2. Variations in ΔG_a^{sp} of diethyl ether adsorbed on carbon fibers (a) and (b) as a function of the temperature for the different models and chromatographic methods.

This large difference between the results from the different molecular models and IGC methods can be clearly seen in Figure 2 for the adsorption of diethyl ether on the two carbon fibers (a) and (b) (the other cases of adsorbed polar molecules are shown in Figures S3 and S4). However, the results in Tables S6 and S7, and Figure 2, Figures S3 and S4 show that the oxidized carbon fibers gave larger specific free enthalpy of adsorption of all used polar molecules, demonstrating the higher Lewis acid–base and amphoteric character of the oxidized carbon fiber.

The previous results presented in Figure 2, Figures S3 and S4, as well as those given in Tables S6 and S7, show that the oxidized carbon fibers exhibited greater specific interactions for all the adsorbed polar solvents. This is due to the oxidization of the surface groups of the carbon fibers that increased the acidic and basic surface sites of the carbon fibers and therefore conducted larger specific free enthalpy of adsorption on the oxidized carbon fibers than on the untreated carbon fibers.

The curves in Figure 2, Figures S3 and S4 giving $\Delta G_a^{sp}(T)$ versus the temperature for the various polar molecules adsorbed on the carbon fibers following the different models and IGC methods led to the determination of the specific enthalpy and entropy of the adsorption of the polar solvents adsorbed on the carbon fibers. The obtained results are presented in the next section.

3.4. Enthalpic and Entropic Acid–Base Constants

The variations in $\Delta G_a^{sp}(T)$ allowed one to obtain the values of specific enthalpy ($-\Delta H_a^{sp}$) and entropy ($-\Delta S_a^{sp}$) of the adsorption of the polar molecules on carbon fibers (a) and (b) for the various models and chromatographic methods. The obtained values of ($-\Delta H_a^{sp}$) are shown in Table 2 and those of ($-\Delta S_a^{sp}$) are shown in Table S8. The determined values of the specific variables varied from one molecular model to the other, with a large deviation. One can conclude that the thermal model gave more accurate results because it took into consideration the thermal effect on the surface area of the organic molecules; this was neglected in the other molecular models (Table 2 and Table S8).

Table 2. Variations in ($-\Delta H_a^{sp}$ in kJ mol^{-1}) as a function of the used models or methods of polar molecules adsorbed on carbon fibers (a) and (b).

Probes	Untreated Carbon Fibers (a)							
	CCl_4	CH_2Cl_2	CHCl_3	Benzene	Ether	THF	EA	Acetone
Kiselev	1.075	1.200	6.011	0.765	12.135	12.456	11.321	16.459
Spherical	4.020	6.751	11.991	12.195	9.371	20.915	18.464	22.925
Geometric	9.512	14.044	41.587	6.642	5.827	13.830	12.562	10.470
VDW	2.523	4.995	19.769	12.685	8.460	20.658	14.704	18.342
R-K	2.601	5.081	19.691	12.494	8.370	20.331	14.483	18.015
Cylindrical	1.541	16.596	38.802	−3.287	4.682	9.464	11.266	9.969
Hamieh model	1.475	1.900	6.011	1.100	13.852	13.093	18.923	13.540
Topological index	7.292	17.167	54.714	5.528	9.132	18.524	9.042	13.164
Deformation polarizability	9.504	0.707	47.722	9.133	11.308	22.853	10.797	15.845
Vapor pressure	−3.789	2.297	44.039	4.700	6.777	14.770	4.576	2.082
Boiling point	−4.167	0.110	41.913	4.990	9.162	13.796	4.262	4.487
DHvap	−3.839	2.382	42.347	4.584	7.495	12.540	2.302	2.438
DHvap(T)	4.069	7.408	53.671	9.034	20.773	22.216	7.813	−4.978
Average values	2.447	6.203	32.944	6.197	9.796	16.573	10.809	10.981

Table 2. Cont.

Oxidized Carbon Fibers (b)								
Probes	CCl ₄	CH ₂ Cl ₂	CHCl ₃	Benzene	Ether	THF	EA	Acetone
Kiselev	4.200	6.958	−18.895	3.170	16.203	20.300	16.512	28.623
Spherical	7.350	13.845	−11.197	16.232	13.477	29.914	24.441	35.723
Geometric	14.586	20.524	15.981	10.199	8.598	21.950	18.548	22.065
VDW	6.045	11.728	−5.159	17.185	12.309	29.983	20.583	31.148
R-K	6.053	11.843	−4.140	16.892	12.292	29.521	20.294	30.633
Cylindrical	4.982	23.658	12.922	−1.537	7.551	16.915	16.682	21.332
Hamieh model	4.782	2.937	11.416	2.931	17.063	20.099	30.039	24.811
Topological index	13.884	25.326	29.357	9.583	12.066	28.413	14.729	27.207
Deformation polarizability	16.481	4.283	20.425	14.201	14.861	33.962	18.262	31.156
Vapor pressure	−0.393	6.459	16.558	8.635	9.739	23.202	11.251	13.724
Boiling point	−0.789	11.799	12.989	8.864	12.220	22.385	9.874	16.157
DHvap	−0.338	6.433	13.555	8.384	9.992	20.772	7.396	13.503
DHvap(T)	7.717	11.939	24.057	13.722	22.735	29.753	14.091	6.858
Average values	6.505	12.133	9.067	9.882	13.008	25.167	17.131	23.303

One also confirmed the larger specific enthalpy of adsorption for all polar molecules in the case of the oxidized carbon fibers, thus proving the higher acid–base characteristics.

The Lewis acid–base constants of the two carbon fibers were determined by using relation (3). The variations in $\left(\frac{-\Delta H_q^{sp}}{AN^i}\right)$ and $\left(\frac{-\Delta S_q^{sp}}{AN^i}\right)$ as a function of $\left(\frac{DN^i}{AN^i}\right)$ are respectively plotted in Figures S5 and S6 for the different IGC methods and models. Figures S5 and S6 show that the linearity of the various curves was not realized for all models and chromatographic methods, except for the Hamieh and Kiselev models. Tables 3 and 4 show the various values of the enthalpic K_A and K_D and entropic ω_A and ω_D acid–base constants of carbon fibers (a) and (b) with the corresponding linear regression coefficient R^2 . The accurate results obtained by using the thermal model showed an important difference from the other models and methods in terms of the acid–base constants. The smaller values of R^2 (<0.500) obtained with the other models led to the belief that these various models cannot be considered accurate. The only interesting result that can be deduced from Tables 3 and 4 is, confirming once again, the important and greater acid–base constants of the oxidized carbon fibers (b) for the different chromatographic methods and models.

Table 3. Values of the acid–base constants K_A , K_D , ω_A , ω_D and R^2 of the untreated carbon fibers (a) with the different acid–base ratios.

Models or Methods	K_A	K_D	K_D/K_A	R^2	$10^{-3}\omega_A$	$10^{-3}\omega_D$	ω_D/ω_A	R^2
Kiselev	0.14	0.29	2.2	0.9705	0.31	0.41	1.3	0.9876
Spherical	0.10	2.53	25.3	0.0475	0.26	4.40	17.0	0.0893
Geometric	0.05	1.99	43.7	0.0366	0.17	2.94	17.7	0.1959
Van der Waals	0.09	2.49	26.7	0.0375	0.27	4.36	16.4	0.0847
Redlich–Kwong	0.09	2.46	27.0	0.0371	0.24	4.04	16.5	0.0844
Cylindrical	0.12	−0.16	−1.4	0.3736	0.30	−0.47	−1.6	0.4863
Hamieh model	0.14	0.44	3.1	0.9252	0.17	0.75	4.5	0.9309

Table 3. Cont.

Models or Methods	K_A	K_D	K_D/K_A	R^2	$10^{-3}\omega_A$	$10^{-3}\omega_D$	ω_D/ω_A	R^2
Topological index	0.11	1.66	15.1	0.2264	0.28	1.09	3.8	0.6131
Deformation polarizability	0.13	2.21	17.3	0.1226	0.30	1.69	5.6	0.4612
Vapor pressure	0.12	0.69	5.9	0.2498	0.24	1.15	4.7	0.4934
Boiling point	0.11	0.76	7.1	0.2089	0.29	0.06	0.2	0.5289
ΔH_{vap}	0.09	0.70	7.5	0.1873	0.27	0.09	0.3	0.5091
$\Delta H_{vap}(T)$	0.14	1.89	13.4	0.1419	0.50	2.43	4.8	0.4308
Average values	0.14	1.28	8.9	0.3193	0.30	1.64	5.5	0.5303

Table 4. Values of the acid–base constants K_A , K_D , ω_A , ω_D and R_2 of the oxidized carbon fibers (b) with the different acid–base ratios.

Models or Methods	K_A	K_D	K_D/K_A	R^2	$10^{-3}\omega_A$	$10^{-3}\omega_D$	ω_D/ω_A	R_2
Kiselev	0.20	0.78	3.9	0.7242	0.34	1.40	4.1	0.8568
Spherical	0.16	3.34	21.2	0.0643	0.30	5.97	20.1	0.0689
Geometric	0.09	2.78	29.7	0.06	0.20	4.01	20.1	0.1061
Van der Waals	0.15	3.37	22.5	0.0515	0.33	5.77	17.5	0.0671
Redlich–Kwong	0.15	0.15	1.0	0.0516	0.30	5.33	17.6	0.0673
Cylindrical	0.18	0.22	1.2	0.7422	0.38	−0.73	−1.9	0.5582
Hamieh model	0.19	1.06	5.4	0.98	0.20	2.52	12.6	0.9244
Topological index	0.17	2.60	15.5	0.1805	0.35	2.68	7.8	0.3816
Deformation polarizability	0.19	3.31	17.4	0.1127	0.38	3.75	9.9	0.2279
Vapor pressure	0.17	1.43	8.3	0.2066	0.37	0.69	1.9	0.4483
Boiling point	0.16	1.54	9.5	0.1829	0.34	1.06	3.2	0.3909
ΔH_{vap}	0.15	1.40	9.5	0.1691	0.31	0.86	2.7	0.3832
$\Delta H_{vap}(T)$	0.18	2.79	15.8	0.106	0.46	4.52	9.8	0.2163
Average values	0.20	2.00	10.2	0.2506	0.35	2.70	7.8	0.3182

For a comparison between the acid–base constants of the untreated and oxidized carbon fibers, Table 5 shows the corresponding acid–base parameters obtained from the thermal model. The results in Table 6 show that the two fiber types are amphoteric with an important basic character. The ratio K_D/K_A is equal to 3.1 (about three times more basic than acidic) for the untreated fibers and 5.4 (more than 5 times more basic than acidic) for the oxidized fibers.

Table 5. Values of K_A , K_D , ω_A and ω_D of the two carbon fibers I and II with the acid–base ratios by using Hamieh thermal model.

Solid Surface	K_A	K_D	K_D/K_A	$10^{-3}\omega_A$	$10^{-3}\omega_D$	ω_D/ω_A
Untreated carbon fibers (a)	0.14	0.44	3.1	0.17	0.75	4.5
Oxidized carbon fibers (b)	0.19	1.06	5.4	0.20	2.52	12.6
Ratio fibers (b)/fibers (a)	1.36	2.41	1.74	1.18	3.36	2.80

Table 6. Values of $(-\Delta G_a^{sp}(T))$ in kJ/mol of the dichloromethane and the ethyl acetate adsorbed on carbon fibers (a) and (b) at various temperatures.

$(-\Delta G_a^{sp}(T))$	Untreated Carbon Fibers		Oxidized Carbon Fibers	
	T(K)	CH ₂ Cl ₂	Ethyl Acetate	CH ₂ Cl ₂
313.15	1.274	10.622	1.274	10.622
323.15	1.254	10.246	1.254	10.246
333.15	1.234	9.881	1.234	9.881
343.15	1.214	9.489	1.214	9.489
353.15	1.194	9.094	1.194	9.094
363.15	1.174	8.746	1.174	8.746
373.15	1.154	8.411	1.154	8.411

One observed that the oxidized fibers are 1.4 times more acidic and 2.4 more basic than the untreated fibers, thus proving the important role of the oxidation of carbon fibers in increasing the acid–base properties. The amphoteric character of the oxidized fibers is about 1.7 more important than that of the untreated fibers.

3.5. Specific and Total Surface Energies of Carbon Fibers

To determine the specific or acid–base surface energy of the studied carbon fibers, one applied the relation of Van Oss et al. [36], given the specific enthalpy of adsorption as a function of the Lewis acid surface energy of the solid surface γ_s^+ and the solvent γ_l^+ , and the corresponding Lewis base surface energy (γ_s^- for the surface and γ_l^- for the solvent):

$$\Delta G_a^{sp}(T) = 2Na \left(\sqrt{\gamma_l^- \gamma_s^+} + \sqrt{\gamma_l^+ \gamma_s^-} \right) \quad (5)$$

In the scale of Van Oss et al. [36], two monopolar solvents, namely, ethyl acetate (EA) and dichloromethane, were used and characterized by

$$\begin{cases} \gamma_{CH_2Cl_2}^+ = 5.2 \text{ mJ/m}^2, \gamma_{CH_2Cl_2}^- = 0 \\ \gamma_{EA}^+ = 0, \gamma_{EA}^- = 19.2 \text{ mJ/m}^2 \end{cases} \quad (6)$$

By combining the two relations (5) and (6), one can determine the Lewis acid and base surface energies of the solid surface, γ_s^+ and γ_s^- , using the following relations:

$$\begin{cases} \gamma_s^+ = \frac{[\Delta G_a^{sp}(T)(EA)]^2}{4N^2[a(EA)]^2 \gamma_{EA}^-} \\ \gamma_s^- = \frac{[\Delta G_a^{sp}(T)(CH_2Cl_2)]^2}{4N^2[a(CH_2Cl_2)]^2 \gamma_{CH_2Cl_2}^+} \end{cases} \quad (7)$$

By using the experimental results obtained from the thermal model for the application of dichloromethane and ethyl acetate on the two carbon fibers, Table 6 shows the corresponding values of $\Delta G_a^{sp}(T)$ at different temperatures.

The values in Table 6 and relations (6) and (7) allowed one to obtain the Lewis acid and base surface energies of the solid surface, γ_s^+ and γ_s^- , as well as the specific surface energy γ_s^{AB} of carbon fibers (a) and (b) by using relation (8):

$$\gamma_s^{AB} = 2\sqrt{\gamma_s^+ \gamma_s^-} \quad (8)$$

The application of relation (8) allowed for the determination of the values of γ_s^{AB} of the carbon fibers at different temperatures. Table 7 shows the different values of γ_s^+ , γ_s^-

and γ_s^{AB} of the untreated and oxidized carbon fibers, γ_s^- and γ_s^{AB} (in mJ/m²) of untreated and oxidized carbon fibers.

Table 7. Values of the specific acid and base surface energy contributions γ_s^+ , γ_s^- and γ_s^{AB} (in mJ/m²) of untreated and oxidized carbon fibers.

In mJ/m ²	Untreated Carbon Fibers			Oxidized Carbon Fibers			
	T(K)	γ_s^-	γ_s^+	γ_s^{AB}	γ_s^-	γ_s^+	γ_s^{AB}
	313.15	0.88	43.88	12.45	1.02	79.70	18.06
	323.15	0.85	40.75	11.79	0.95	74.19	16.77
	333.15	0.82	37.82	11.17	0.88	68.96	15.54
	343.15	0.80	34.81	10.53	0.81	63.83	14.35
	353.15	0.77	31.91	9.91	0.74	58.79	13.20
	363.15	0.74	29.45	9.35	0.68	53.86	12.08
	373.15	0.72	27.19	8.82	0.62	49.06	11.00

The obtained values of the specific surface energy γ_s^{AB} given in Table 7 show that γ_s^{AB} of the oxidized fibers is obviously larger (about 1.5 times) than that of the untreated fibers. The total surface energy $\gamma_s^{tot.}$ of the fibers can then be obtained by using relation (9):

$$\gamma_s^{tot.} = \gamma_s^d + \gamma_s^{AB} \quad (9)$$

The above results of the specific acid–base surface energies of the carbon fibers allowed for the total surface energy of the fibers to be determined by summing the specific surface energy and the dispersive surface energy of the carbon fibers using the results obtained with the thermal model of the two cases where the surface areas of the molecules were calculated by using the PTFE substrate as a model solid (thermal model 1) or PE surface (thermal model 2). The results are given in Table 8.

Table 8. Values of the dispersive γ_s^d and total $\gamma_s^{tot.}$ surface energies (in mJ/m²) of untreated and oxidized carbon fibers by using the two thermal models.

In mJ/m ²	Thermal Model 1				
	T(K)	$\gamma_s^d(Fiber (a))$	$\gamma_s^{tot.}(Fiber (a))$	$\gamma_s^d(Fiber (b))$	$\gamma_s^{tot.}(Fiber (b))$
	313.15	74.9	87.3	74.3	92.3
	323.15	71.0	82.8	69.1	85.8
	333.15	67.6	78.7	64.1	79.7
	343.15	63.8	74.3	59.3	73.7
	353.15	60.2	70.2	54.6	67.8
	363.15	57.9	67.2	50.0	62.1
	373.15	56.1	64.9	45.5	56.5
In mJ/m ²	Thermal Model 2				
	T(K)	$\gamma_s^d(Fiber (a))$	$\gamma_s^{tot.}(Fiber (a))$	$\gamma_s^d(Fiber (b))$	$\gamma_s^{tot.}(Fiber (b))$
	313.15	56.3	68.8	55.9	74.0
	323.15	53.0	64.8	51.5	68.3
	333.15	49.9	61.1	47.4	62.9
	343.15	46.6	57.2	43.3	57.6

Table 8. Cont.

In mJ/m^2	Thermal Model 2			
T(K)	$\gamma_s^d(\text{Fiber (a)})$	$\gamma_s^{\text{tot.}}(\text{Fiber (a)})$	$\gamma_s^d(\text{Fiber (b)})$	$\gamma_s^{\text{tot.}}(\text{Fiber (b)})$
353.15	43.5	53.4	39.2	52.4
363.15	41.1	50.4	35.2	47.3
373.15	38.9	47.7	31.3	42.3

The results in Table 8 show that the two thermal models reached the same conclusion of a greater total surface energy of the oxidized carbon fiber (b) by about 10% more than that of the untreated carbon fibers, certainly due to the important difference in the values of the specific surface energy between the two fibers because of the increase in the acid–base site numbers in the oxidized fibers. However, when comparing between the magnitudes of the specific acid–base surface energy and the dispersive surface energy of the fibers, one observed that the ratio of γ_s^{AB}/γ_s^d varied between 14% and 20% for the untreated fibers and between 25% and 30% for the oxidized fibers (Figure 3). This is certainly due to the greater percentage of oxygen present in the oxidized form. The results of the chemical analysis of the two carbon fibers determined using XPS measurements are presented in Table 9.

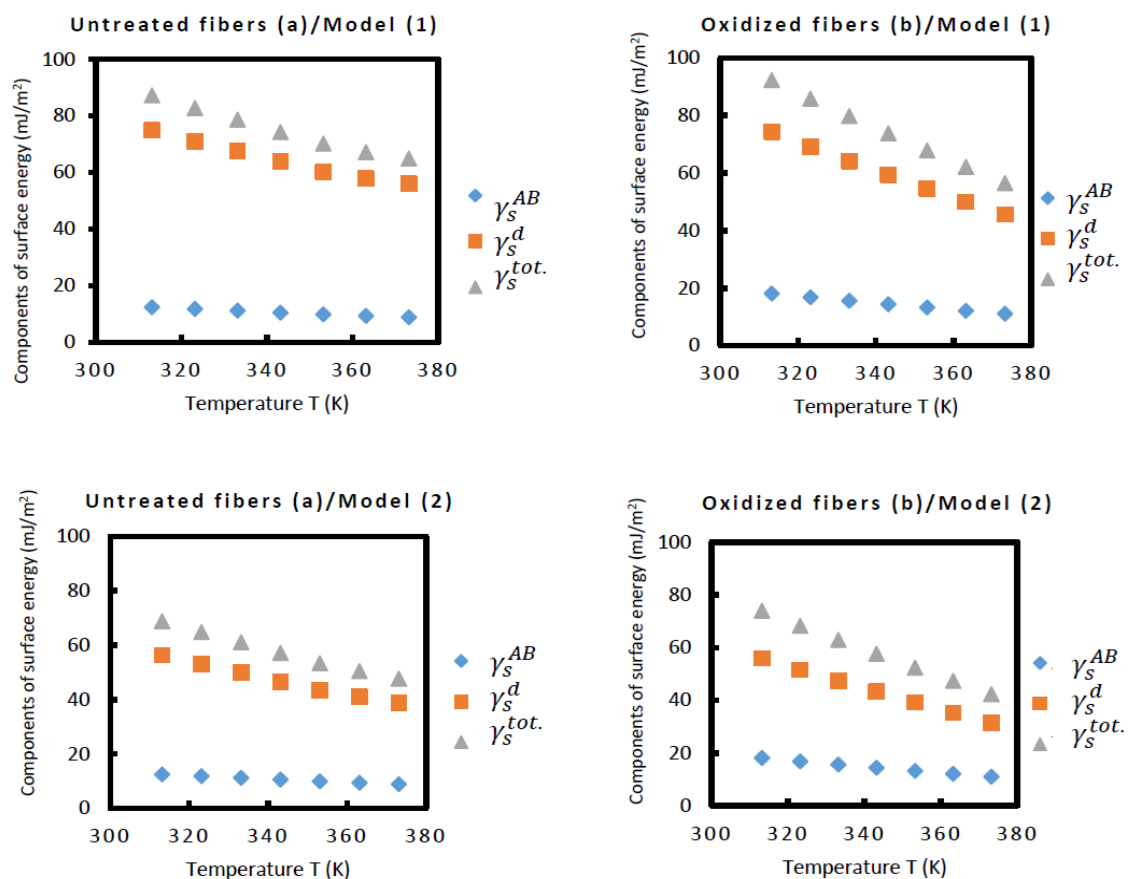


Figure 3. Evolution of the different components of the surface energy of the two carbon fibers as a function of the temperature.

Table 9. Element percentages of the untreated and oxidized fibers.

Carbon Fiber	% C	% O	% N	O/C
Untreated	93.12	5.10	1.78	0.055
Oxidized	87.31	11.07	1.62	0.127

3.6. Comparison with Other Results in the Literature

Many papers have been devoted to the determination of the surface physicochemical properties of activated carbons or carbon fibers by using the inverse gas chromatography technique at infinite dilution.

Schultz et al. [15] determined the dispersive energy components of untreated and oxidized carbon fibers and obtained the values of $\gamma_s^d = 50 \text{ mJ/m}^2$ and $\gamma_s^d = 49 \text{ mJ/m}^2$ at only 320.6 K, respectively. These values cannot be taken into consideration because, as previously mentioned, these authors neglected the thermal effect on the surface area of the solvents and on their surface tensions. Consequently, the values of the acid–base constants cannot be considered accurate. In fact, for the two fiber types, they obtained a more acidic surface, with $K_A = 6.5$ and $K_D = 1.5$ for the untreated carbon fiber and $K_A = 10.0$ and $K_D = 3.2$ for the oxidized carbon fiber, while all other models and chromatographic methods showed a higher basic surface for carbon fibers. Later, Menzel et al. [37] found a dispersive surface energy of untreated and oxidized carbon nanotubes equal to $\gamma_s^d = 94 \text{ mJ/m}^2$. In a recent study, Pal et al. [19] found a higher basicity surface of surface-treated activated carbons, with K_A ranging from 0.042 to 0.056 and K_D ranging from 0.129 to 0.205. They also determined the dispersive surface energy of activated carbons at 140 °C and obtained the values of γ_s^d for different activated carbons, ranging between $\gamma_s^d = 213 \text{ mJ/m}^2$ and $\gamma_s^d = 293 \text{ mJ/m}^2$ depending on the surface coverage and the activated carbons. However, Pal et al. [19] did not take into account the thermal effect or the variations in the surface tension γ_l^d of the solvents as a function of the temperature, and they further took $\left(\frac{-\Delta G_a^{sp}}{AN^t}\right)$ instead of $\left(\frac{-\Delta H_a^{sp}}{AN^t}\right)$ by confusing the specific free surface energy ΔG_a^{sp} and the specific enthalpy ΔH_a^{sp} by neglecting the entropic contribution that was shown to be very important in such cases. By studying various carbon fibers, Liu et al. [18] found a dispersive surface energy of the fibers equal to 40 mJ/m^2 and a polar contribution equal to 9 mJ/m^2 by using the same previous errors previously mentioned. The superiority of our thermal models resides in the correction of the various values of the surface thermodynamic parameters and variables.

4. Conclusions

In this study, we were interested in the determination of the surface physicochemical properties of untreated and oxidized carbon fibers using the inverse gas chromatography technique at infinite dilution. Experimental measurements allowed for the retention volume of n-alkanes and polar solvents adsorbed on the carbon fibers to be determined. The variations in $RT \ln(Vn)$ of the adsorbed organic molecules as a function of the temperature led to the determination of the dispersive component of the surface energy of the two carbon fibers and the specific and Lewis acid–base interactions. The results show comparable values of γ_s^d for the two studied carbon fibers. The specific free energy $\Delta G_a^{sp}(T)$ of the adsorption of the polar molecules was determined and showed larger values in the case of the oxidized carbon fibers. The variations in $\Delta G_a^{sp}(T)$ versus the temperature allowed for obtaining the values of the specific enthalpy $\left(-\Delta H_a^{sp}\right)$ and entropy $\left(-\Delta S_a^{sp}\right)$ of the adsorption of the polar molecules on carbon fibers (a) and (b) for the various models and chromatographic methods. The larger values of $\left(-\Delta H_a^{sp}\right)$ of the different polar solvents for the oxidized fibers showed that the acid–base site number was greater than that of the untreated fibers, due to the oxidization of the surface groups of the carbon fibers.

The determination of the Lewis acid–base constants indicated that the oxidized fibers were 1.4 times more acidic and 2.4 more basic than the untreated fibers. This proved the important role of the oxidation of the carbon fibers by increasing the acid–base properties. The amphoteric character of the oxidized fibers was shown to be 1.7 more important than that of the untreated fibers.

One also determined the Lewis acid and base surface energies of the solid surface, γ_s^+ and γ_s^- , and therefore the values of the specific acid–base surface energy γ_s^{AB} of the carbon fibers at different temperatures. One deduced that the specific surface energy γ_s^{AB} of the oxidized fibers was larger (by about 1.5 times) than that of the untreated fibers, confirming the results previously obtained on the strong acid–base interactions of the oxidized carbon fibers with the various polar molecules.

This study clearly shows the non-validity of all methods and models that neglected the effect of temperature on both the surface areas and the surface tensions of organic solvents. A protocol of applied chromatographic methods has to be used while taking into account the thermal effect in all calculations of the various surface thermodynamic parameters and trying to correct the different hypotheses that have been applied for more than forty years.

Supplementary Materials: The following supporting information can be downloaded at: <https://www.mdpi.com/article/10.3390/cryst14010028/s1>, Figure S1. Variations in $RT\ln Vn$ of the various solvents adsorbed on untreated carbon fibers (a) as a function of the temperature. Figure S2. Variations in $RT\ln Vn$ of the various solvents adsorbed on oxidized carbon fibers (b) as a function of the temperature. Figure S3. Variations in ΔG_a^{sp} of the various solvents adsorbed on untreated carbon fibers as a function of the temperature for the different models and chromatographic methods. Figure S4. Variations in ΔG_a^{sp} of the various solvents adsorbed on oxidized carbon as a function of the temperature for the different models and chromatographic methods. Figure S5. Variations in $\left(\frac{-\Delta H_a^{sp}}{AN^d}\right)$ as a function of $\left(\frac{DN^d}{AN^d}\right)$ for different molecular models and IGC methods for carbon fibers (a) and (b). Figure S6. Variations in $\left(\frac{-\Delta S_a^{sp}}{AN^d}\right)$ as a function of $\left(\frac{DN^d}{AN^d}\right)$ by using the various molecular models and IGC methods for carbon fibers (a) and (b). Table S1. Surface areas of various molecules (in \AA^2) given by the Van der Waals (VDW), Redlich–Kwong (R-K), Kiselev, geometric, cylindrical or spherical models. Table S2. Values of the surface entropy ε_X (in $\text{mJ}/(\text{K} \times \text{m}^2)$) and $\gamma_{iX}^d(0\text{K})$ (in mJ/m^2) of the n-alkanes. Table S3. Normalized donor and acceptor numbers of some polar molecules. Table S4. Values of $RT\ln Vn$ (in kJ/mol) of the various polar solvents adsorbed on untreated carbon fibers (a) as a function of the temperature. Table S5. Values of $RT\ln Vn$ (in kJ/mol) of the various polar solvents adsorbed on oxidized carbon fibers (b) as a function of the temperature. Table S6. Values of $(\Delta G_a^{sp}(T))$ (in kJ/mol) of the various polar solvents adsorbed on untreated carbon fibers (a) as a function of the temperature by using the various models and IGC methods. Table S7. Values of $(\Delta G_a^{sp}(T))$ (in kJ/mol) of the various polar solvents on oxidized carbon fibers (b) as a function of the temperature by using the various models and IGC methods. Table S8. Variations in $(-\Delta S_a^{sp})$ in $\text{kJ mol}^{-1} \text{mol}^{-1}$ as a function of the used models or methods of polar molecules adsorbed on carbon fibers (a) and (b).

Funding: This research received no external funding.

Data Availability Statement: The data are contained within the Supplementary Material.

Conflicts of Interest: The author declares no conflicts of interest.

References

- Collins, M.N.; Culebras, M.; Ren, G. Chapter 8—The use of lignin as a precursor for carbon fiber–reinforced composites. In *Micro and Nanolignin in Aqueous Dispersions and Polymers*; Puglia, D., Santulli, C., Sarasini, F., Eds.; Elsevier: Amsterdam, The Netherlands, 2022; pp. 237–250. ISBN 9780128237021. [[CrossRef](#)]
- Morgan, P. *Carbon Fibers and Their Composites*; CRC Press: Boca Raton, FL, USA, 2005; 1200p, ISBN 9780429116827. [[CrossRef](#)]
- Park, S.J. *Carbon Fibers*; Springer Series in Materials Science (SSMATERIALS, Volume 210); Springer: Dordrecht, The Netherlands, 2015; 330p. [[CrossRef](#)]
- Frank, E.; Steudle, L.M.; Ingildeev, D.; Spörl, J.M.; Buchmeiser, M.R. Carbon fibers: Precursor systems, processing, structure, and properties. *Angew. Chem. Int. Ed.* **2014**, *53*, 5262–5298. [[CrossRef](#)] [[PubMed](#)]

5. Peijs, T.; Kirschbaum, R.; Jan Lemstra, P. Chapter 5: A critical review of carbon fiber and related products from an industrial perspective. *Adv. Ind. Eng. Polym. Res.* **2022**, *5*, 90–106. [[CrossRef](#)]
6. Roberts, T. *The Carbon Fiber Industry: Global Strategic Market Evaluation 2006–2010*; Materials Technology Publications: Watford, UK, 2006; Volume 10, pp. 93–177.
7. Red, C. Aerospace will continue to lead advanced composites market in 2006. *Compos. Manuf.* **2006**, *7*, 24–33.
8. Papirer, E.; Brendlé, E.; Ozil, F.; Balard, H. Comparison of the surface properties of graphite, carbon black and fullerene samples, measured by inverse gas chromatography. *Carbon* **1999**, *37*, 1265–1274. [[CrossRef](#)]
9. Chung, D.L. *Carbon Fiber Composites*; Butterworth-Heinemann: Boston, MA, USA, 1994; pp. 3–65.
10. Donnet, J.B.; Bansal, R.C. *Carbon Fibers*, 2nd ed.; Marcel Dekker: New York, NY, USA, 1990; pp. 1–145.
11. Friedlander, H.N.; Peebles, L.H., Jr.; Brandrup, J.; Kirby, J.R. On the chromophore of polyacrylonitrile. VI. Mechanism of color formation in polyacrylonitrile. *Macromolecules* **1968**, *1*, 79–86. [[CrossRef](#)]
12. Huang, X. Fabrication and Properties of Carbon Fibers. *Materials* **2009**, *2*, 2369–2403. [[CrossRef](#)]
13. Qiao, Z.; Ding, C. Recent progress in carbon fibers for boosting electrocatalytic energy conversion. *Ionics* **2022**, *28*, 5259–5273. [[CrossRef](#)]
14. Schultz, J.; Lavielle, L.; Martin, C. The role of the interface in carbon fibre-epoxy composites. *J. Adhes.* **1987**, *23*, 45–60. [[CrossRef](#)]
15. Schultz, J.; Lavielle, L.; Martin, C. Propriétés de surface des fibres de carbone déterminées par chromatographie gazeuse inverse. *J. Chim. Phys.* **1987**, *84*, 231. [[CrossRef](#)]
16. Hamieh, T. Surface acid-base properties of carbon fibres. *Adv. Powder Technol.* **1997**, *8*, 279–289. [[CrossRef](#)]
17. Le Vu, H.; Nguyen, S.H.; Dang, K.Q.; Pham, C.V.; Le, H.T. The Effect of Oxidation Temperature on Activating Commercial Viscose Rayon-Based Carbon Fibers to Make the Activated Carbon Fibers (ACFs). *Mater. Sci. Forum* **2020**, *985*, 171–176. [[CrossRef](#)]
18. Liu, Y.; Gu, Y.; Wang, S.; Li, M. Optimization for testing conditions of inverse gas chromatography and surface energies of various carbon fiber bundles. *Carbon Lett.* **2023**, *33*, 909–920. [[CrossRef](#)]
19. Pal, A.; Kondor, A.; Mitra, S.; Thua, K.; Harish, S.; Saha, B.B. On surface energy and acid–base properties of highly porous parent and surface treated activated carbons using inverse gas chromatography. *J. Ind. Eng. Chem.* **2019**, *69*, 432–443. [[CrossRef](#)]
20. Hamieh, T. Study of the temperature effect on the surface area of model organic molecules, the dispersive surface energy and the surface properties of solids by inverse gas chromatography. *J. Chromatogr. A* **2020**, *1627*, 461372. [[CrossRef](#)] [[PubMed](#)]
21. Hamieh, T.; Ahmad, A.A.; Roques-Carmes, T.; Toufaily, J. New approach to determine the surface and interface thermodynamic properties of H- β -zeolite/rhodium catalysts by inverse gas chromatography at infinite dilution. *Sci. Rep.* **2020**, *10*, 20894. [[CrossRef](#)] [[PubMed](#)]
22. Hamieh, T. New methodology to study the dispersive component of the surface energy and acid–base properties of silica particles by inverse gas chromatography at infinite dilution. *J. Chromatogr. Sci.* **2022**, *60*, 126–142. [[CrossRef](#)]
23. Hamieh, T. New Physicochemical Methodology for the Determination of the Surface Thermodynamic Properties of Solid Particles. *AppliedChem* **2023**, *3*, 229–255. [[CrossRef](#)]
24. Hamieh, T.; Schultz, J. New approach to characterise physicochemical properties of solid substrates by inverse gas chromatography at infinite dilution. I. Some new methods to determine the surface areas of some molecules adsorbed on solid surfaces. *J. Chromatogr. A* **2002**, *969*, 17–47. [[CrossRef](#)]
25. Sawyer, D.T.; Brookman, D.J. Thermodynamically based gas chromatographic retention index for organic molecules using salt-modified aluminas and porous silica beads. *Anal. Chem.* **1968**, *40*, 1847–1850. [[CrossRef](#)]
26. Saint-Flour, C.; Papirer, E. Gas-solid chromatography. A method of measuring surface free energy characteristics of short carbon fibers. 1. Through adsorption isotherms. *Ind. Eng. Chem. Prod. Res. Dev.* **1982**, *21*, 337–341. [[CrossRef](#)]
27. Saint-Flour, C.; Papirer, E. Gas-solid chromatography: Method of measuring surface free energy characteristics of short fibers. 2. Through retention volumes measured near zero surface coverage. *Ind. Eng. Chem. Prod. Res. Dev.* **1982**, *21*, 666–669. [[CrossRef](#)]
28. Donnet, J.-B.; Park, S.; Balard, H. Evaluation of specific interactions of solid surfaces by inverse gas chromatography. *Chromatographia* **1991**, *31*, 434–440. [[CrossRef](#)]
29. Chehimi, M.M.; Abel, M.-L.; Perruchot, C.; Delamar, M.; Lascelles, S.F.; Armes, S.P. The determination of the surface energy of conducting polymers by inverse gas chromatography at infinite dilution. *Synth. Met.* **1999**, *104*, 51–59. [[CrossRef](#)]
30. Chehimi, M.M.; Pigois-Landureau, E. Determination of acid–base properties of solid materials by inverse gas chromatography at infinite dilution. A novel empirical method based on the dispersive contribution to the heat of vaporization of probes. *J. Mater. Chem.* **1994**, *4*, 741–745. [[CrossRef](#)]
31. Brendlé, E.; Papirer, E. A new topological index for molecular probes used in inverse gas chromatography for the surface nanorugosity evaluation, 2. Application for the Evaluation of the Solid Surface Specific Interaction Potential. *J. Colloid Interface Sci.* **1997**, *194*, 217–224. [[CrossRef](#)]
32. Brendlé, E.; Papirer, E. A new topological index for molecular probes used in inverse gas chromatography for the surface nanorugosity evaluation, 1. Method of Evaluation. *J. Colloid Interface Sci.* **1997**, *194*, 207–216. [[CrossRef](#)]
33. Gutmann, V. *The Donor-acceptor Approach to Molecular Interactions*; Plenum: New York, NY, USA, 1978.
34. Dorris, G.M.; Gray, D.G. Adsorption of n-alkanes at zero surface coverage on cellulose paper and wood fibers. *J. Colloid Interface Sci.* **1980**, *77*, 353–362. [[CrossRef](#)]
35. Fowkes, F.M. *Surface and Interfacial Aspects of Biomedical Polymers*. Andrade, J.D., Ed.; Plenum Press: New York, NY, USA, 1985; Volume I, pp. 337–372.

36. Van Oss, C.J.; Good, R.J.; Chaudhury, M.K. Additive and nonadditive surface tension components and the interpretation of contact angles. *Langmuir* **1988**, *4*, 884. [[CrossRef](#)]
37. RMenzel; Bismarck, A.; Shaffer, M.S.P. Deconvolution of the structural and chemical surface properties of carbon nanotubes by inverse gas chromatography. *Carbon* **2012**, *50*, 3416–3421. [[CrossRef](#)]

Disclaimer/Publisher’s Note: The statements, opinions and data contained in all publications are solely those of the individual author(s) and contributor(s) and not of MDPI and/or the editor(s). MDPI and/or the editor(s) disclaim responsibility for any injury to people or property resulting from any ideas, methods, instructions or products referred to in the content.